Epithelial Cell Extrusion Leads to Breaches in the Intestinal Epithelium

Julia J. Liu, MSc, MD, Elisabeth M. Davis, PhD,† Eytan Wine, MD, PhD,‡ Yuefei Lou, MD, MSc,* Jan K. Rudzinski, BSc,§ Misagh Alipour,* Pierre Boulanger, PhD,‖ Aducio L. Thiesen, MD, PhD,¶ Consolato Sergi, MD, PhD,¶ Richard N. Fedorak, MD,* Daniel Muruve, MD,§ Karen L. Madsen, PhD,* and Randall T. Irvin, PhD†*

Background: Two distinct forms of intestinal epithelial cell (IEC) extrusion are described: 1 with preserved epithelial integrity and 1 that introduced breaches in the epithelial lining. In this study, we sought to determine the mechanism underlying the IEC extrusion that alters the permeability of the gut epithelium.

Methods: IEC extrusions in polarized T84 monolayer were induced with nigericin. Epithelial permeability was assessed with transepithelial electrical resistance and movements of latex microspheres and green fluorescent protein–transfected *Escherichia coli* across the monolayer. In vivo IEC extrusion was modulated in wild-type and a colitic (interleukin-10 knock-out) mouse model with caspase-1 activation and inhibition. Luminal aspirates and mucosal biopsies from control patients and patients with inflammatory bowel disease were analyzed for caspase-1 and caspase-3&7 activation.

Results: Caspase-1–induced IEC extrusion in T84 monolayers resulted in dose-dependent and time-dependent barrier dysfunction, reversible with caspase-1 inhibition. Moreover, the movements of microspheres and microbes across the treated epithelial monolayers were observed. Increased caspase-1–mediated IEC extrusion in interleukin-10 knock-out mice corresponded to enhanced permeation of dextran, microspheres, and translocation of *E. coli* compared with wild type. Caspase-1 inhibition in interleukin-10 knock-out mice resulted in a time-dependent reduction in cell extrusion and normalization of permeability to microspheres. Increased IEC extrusion in wild-type mice was induced with caspase-1 activation. In human luminal aspirates, the ratio of positively stained caspase-1 to caspase-3&7 cells were 1:1 and 2:1 in control patients and patients with inflammatory bowel disease, respectively; these observations were confirmed by cytochemical analysis of mucosal biopsies.

Conclusions: IEC extrusion mediated by caspase-1 activation contributes to altered intestinal permeability in vitro and in vivo.

(Inflamm Bowel Dis 2013;0:1–10)

Key Words: intestinal epithelial cells, barrier function, epithelial integrity, caspase-1, interleukin-1 beta, pyroptosis, inflammasome, cell extrusion, bacteria, mucosa, inflammatory bowel disease, confocal endomicroscopy, small intestine

Two distinct forms of intestinal epithelial cell (IEC) extrusions have been previously reported in the mammalian intestine[1]: 1 mediated by apoptosis with preserved barrier function[2,3] and the second form of cell extrusion described as cell death reminiscent of necrosis that was associated with compromised epithelial integrity.[4] Apoptosis-mediated IEC extrusions have been shown to occur in villus-like organoids created from a single stem cell that could be identified by stain for activated caspase-3.[5] In an elegant study of human intestinal resection specimens, apoptosis accounted for 44% of extruded cells in the intestine.[6] The second form of cell shedding described as detachment-induced apoptosis or anoikis in some reports displayed morphological features of distinct chromatin condensation in the nuclei, intact mitochondria, and small or large clear vacuoles in the cytoplasm.[7] The molecular mechanism underlying this form of cell extrusion is unknown.

A study revealed that rapidly replicating intracellular *Salmonella enterica* could induce IEC extrusion through caspase-1 activation in vitro and in vivo.[8] Caspase-1 is a cysteine protease that cleaves interleukin (IL)-1β and IL-18 precursors to active form.[9] Caspase-1 activation can be mediated by the inflammasome[10]—a multimolecular cytosolic complex that can be induced by microbial or nonmicrobial stimuli.[11] Inflammatory cell death mediated by caspase-1 activation is known as pyroptosis[12] and was first observed in myeloid cells.[13,14] Compared with classical caspase-3–mediated apoptosis, pyroptosis is characterized by morphological features of cell swelling with preserved nuclear and mitochondrial

Received for publication June 17, 2012; Accepted August 6, 2012.

From the *Gastroenterology Division; †Department of Medical Microbiology and Immunology; ‡Department of Pediatrics, University of Alberta, Edmonton, Alberta, Canada; §Department of Medicine, University of Calgary, Calgary, Alberta, Canada; ‖Department of Computing Sciencel; and ¶Department of Laboratory Medicine and Pathology, University of Alberta, Edmonton, Alberta, Canada.

Supported by the Canadian Institute of Health Research (J.J.L.), Canadian Association of Gastroenterology (J.J.L.), the Canadian Foundation for Innovations (R.N.F.), and Natural Sciences and Engineering Research Council of Canada (R.T.I.).

The authors have no conflicts of interest to disclose.

Reprints: Julia J. Liu, MSc, MD, Division of Gastroenterology, 1–10 Zeidler Ledcor Centre, University of Alberta, Edmonton, Alberta, Canada T6G 2X8 (e-mail: julia.liu@ualberta.ca).

DOI 10.1097/MIB.0b013e3182807600

Published online.

integrity, accompanied by release of active inflammatory cytokines IL-1β and IL-18.[15,16] IL-1β is a potent proinflammatory cytokine implicated in mucosal inflammation[17] and contributes to the sustained inflammatory responses in inflammatory bowel disease (IBD). Increased IL-1β production in mucosal tissues from patients with IBD has been consistently reported.[18–20] Upstream to IL-1β, Nlrp3, an inflammasome component, is found to be a regulator of intestinal homeostasis,[21,22] and its polymorphisms has been identified as a candidate gene for Crohn's disease.[23]

Luminal commensal bacteria are believed to be the drivers of chronic mucosal inflammation in IBD.[24] In patients with IBD, increased intramucosal and lymph node bacteria[25–27] suggest enhanced translocation of microbes across the epithelial lining. Intolerance to host's own gut microflora reported in patients with IBD further supports the notion of abnormal host–microbial interaction in the intestinal mucosa of these patients.[28] However, the mechanism by which whole bacteria can gain entry into the host and interact with the immune system remains unknown.[29] In rodent models, extrusion of an IEC can leave a gap or discontinuity in the epithelial lining that take up to 12 minutes to resolve and may compromise the barrier function.[30] Identification of such epithelial gaps in the human intestine was reported using confocal laser endomicroscopy[31] and seemed to be increased in patients with IBD.[32] The cause of this increase in epithelial gaps is unknown.

In the present study, we explored the molecular mechanism of IEC extrusion that leads to compromised epithelial integrity and found that caspase-1 activation in IECs results in cell shedding that leads to breaches in the intestinal epithelium. This form of cell extrusion seems to be significantly increased in patients with IBD and may be partly responsible for increased epithelial gaps observed.

MATERIALS AND METHODS

Mice

IL-10 knock-out (KO) mice (Jackson Laboratories, Bar Harbor, ME) and the background 129/SvEv mice (Taconic Farms, Inc., Cambridge City, IN) bred in our animal facilities for at least 10 generations between 24 and 28 weeks old were used for all experiments. Mice were housed in conventional housing facility with light and dark cycles. The Animal Care and Use Committee for Health Sciences at the University of Alberta approved the animal protocol.

Patient Samples

The Human Ethics Research Review Board at the University of Alberta reviewed and approved the study protocol, and the study was registered at ClinicalTrial.Gov (NCT00988273). Patients undergoing colonoscopy provided written informed consent to participate in the study. In patients with IBD (N = 11, 6 Crohn's disease and 5 ulcerative colitis) and asymptomatic control patients (N = 8) undergoing colonoscopy, luminal aspirates from normal-appearing terminal ileum were collected after gentle washing of the intestinal surface with 0.9% NaCl solution using a previously described method[7] and were analyzed immediately (<15 minutes). Cytology blocks were prepared from 25 mL luminal aspirates collected after saline wash and stained with hematoxylin and eosin for morphological identification of epithelial or immune cells. For FLICA staining, cells from 5 mL aspirate fluid were immobilized onto a 25-mm polycarbonate Membra-film Nuclepore membrane with 5.0 μM pore size (Whatman; GE Healthcare Life Sciences, Piscataway, NJ) using vacuum filtration and washed by the filtration of an additional 20 mL phosphate-buffered saline (PBS) (pH 7.4) containing 0.5% (wt/vol) bovine albumin serum (BSA). Fluorescent active site–directed irreversible inhibitors' specific activated caspase-1 and caspase-3&7 (Carboxyfluorescein FLICA Apoptosis Detection Kit; Immunochemistry Technologies LLC, Bloomington, MN) were used to stain aspirated cells directly on the Nuclepore membrane. The membrane with immobilized aspirated cells was cut in half and stained with 1:700 dilution of FAM-YVAD-FMK (FLICA-1) stain to detect activated caspase-1 or FAM-DEVD-FMK (FLICA-3&7) stain to detect activated caspase-3&7. Four mucosal biopsy samples from normal-appearing terminal ileum were obtained for analysis (controls, N = 3; IBD, N = 3), 2 biopsy samples were placed in liquid nitrogen, and stored at −80°C until use for cytokines assays. Two biopsy samples were embedded in OCT (Tissue-Tek, Torrance, CA), placed in liquid nitrogen, and stored at −80°C until sections were prepared.

Reagents

Nigericin (Invitrogen, Burlington, Canada), Ac-YVAD-CMK (Alexis Biochemicals, Farmingdale, NY), and varying diameters (0.5–6 μm) of Fluoresbrite Yellow Green Carboxylate Microspheres (Polysciences, Inc., Warrington, PA) were purchased. Type IV pili were prepared from *Pseudomonas aeruginosa* strain K with a method previously described,[33] characterized in terms of purity through sodium dodecyl sulfate–polyacrylamide gel electrophoresis, ability to bind to asialo-GM1 but not to GM1, and ability to bind to stainless steel.[33] The pili preparation contained low amounts of *P. aeruginosa* serotype 05 lipopolysaccharide that was not detectable on silver-stained sodium dodecyl sulfate–polyacrylamide gel electrophoresis gels. *Escherichia coli* TMW2.497 was an *E. coli* JM109 derivative carrying the gene coding for green fluorescent protein on plasmid pQBI-63 (courtesy of Dr M. Gantzle).[34]

Cell Culture and Measurement of In Vitro Permeability

T84 human colon cancer epithelial cells were maintained in tissue culture plates (10 cm) in Dulbecco's minimal essential medium/F-12, 10% (vol/vol) heat-inactivated fetal bovine serum, and 1% (wt/vol) penicillin–streptomycin. The cells were plated onto Transwells (2×10^5 cells/well, 6.5 mm diameter; 0.4 μm pore size; Corning Life Sciences, Tewksbury, MA) and grown until development of apical junctional complexes (as indicated by a transepithelial electrical resistance [TER] of >2000 Ω/cm^2) for studies. For caspase-1 inhibition experiment, before nigericin treatment, the tissue culture medium was removed and fresh medium with 50 μM caspase-1 inhibitor (Ac-YVAD-CMK) was introduced. Nigericin

(10, 25, and 50 μM) was added to both the apical and basolateral aspect of the Transwell. TER was measured at before and 3 hours after nigericin treatment using a Millicell-ERS Voltmeter and chopstick electrodes (Millipore, Bedford, MA). For microspheres and *E. coli* experiments, after overnight incubation with nigericin, 10^7/mL of 1-μm microspheres or 10^9/mL *E. coli* TMW2.497 was added to the apical aspect of Transwell. One hour after incubation with the microspheres or *E. coli*, the cells were fixed in cold methanol for 5 minutes. Cells were then permeabilized in 0.2% (vol/vol) Triton X-100 for 15 minutes and blocked for 1 hour in PBS with 0.2% (vol/vol) goat serum and 1% (wt/vol) BSA.

Protein Extraction

Human biopsy samples and rodent ileal tissues were homogenized in lysis buffer (0.01 M PBS, 0.5% [vol/vol] Tween 20, and Halt protease inhibitor [containing dimethyl sulfoxide and 4-(2-aminoethyl)-benzenesulfonyl fluoride]; Thermo Scientific, Pittsburgh, PA) on ice for protein extraction. Protein-containing supernatant was separated by centrifugation at 13,000*g* for 30 minutes at 4°C and stored at −70°C until analysis.

Cytokine Expression Assays

Concentration of active IL-1β from human samples was measured with Human IL-1β Ultra-Sensitive Kit (Meso Scale Discovery, Gaithersburg, MD). Active IL-1β expression in mouse intestinal tissue was measured with Mouse ProInflammatory 7-Plex Ultra-Sensitive Kit (Meso Scale Discovery). Resulting cytokines were normalized for the total protein content of each individual sample as determined by bicinchoninic acid assay (Pierce, Rockford, IL).

Western Blot Analysis

Human biopsy tissues, mouse ileal mucosal scrapings, and T84 cells were lysed in M-PER Mammalian Protein Extraction Reagent (Thermo Scientific) containing protease inhibitors. Total cellular lysates (50 μg protein normalized for the samples) were loaded in 15% sodium dodecyl sulfate–polyacrylamide gel electrophoresis gel and underwent subsequent electrophoretic transfer of proteins to a nitrocellulose membrane. Membranes were blocked with ODYSSEY blocking Buffer (InfraRed Imaging System, Marysville, OH) for 1 hour at room temperature (RT) and probed overnight at 4°C with IL-1β antibody (Cell Signaling Technology, Danvers, MA) or caspase-1 antibody (Abcam, Cambridge, MA), with β-actin antibody serving as a loading control (Cell Signaling Technology). After washing, membranes were incubated with the fluorescent secondary antibodies for 1 hour at RT and analyzed by the LI-COR Odyssey (InfraRed Imaging System).

Immunofluorescence Analysis of Cell Culture and Intestinal Samples

Cell culture samples from caspase-1 activation and permeability experiments were fixed in cold methanol for 5 minutes, incubated with the primary rabbit anti-ZO-1 antibody (Invitrogen) overnight at 4°C. After washing, the cells were incubated with either 1:150 dilution of FLICA-1 stain for caspase-1 activation or goat anti-rabbit IgG Alex546 antibody (Invitrogen) and counterstained with 4′,6-diamidino-2-phenylindole (DAPI). Membranes supporting the monolayers were then excised and mounted onto glass slides (DakoCytomation Mounting Medium, Carpinteria, CA). Frozen human biopsy samples were sectioned at 5 μm, air dried, and acetone-fixed before staining with 1:50 dilution of FLICA-1 for activated caspases-1 and with 1:50 dilution of FLICA-3&7 for activated caspase-3&7 (Immunochemistry Technologies LLC). Sections were then postfixed with 4% paraformaldehyde for 15 minutes at RT and stained with rhodamine-phalloidin (Invitrogen) for F-actin and DAPI for nuclei.

Rodent intestinal frozen tissue blocks were sectioned at 5 μm using cryostat, placed in RT for 30 minutes, fixed in 4% paraformaldehyde freshly prepared in PBS for 30 minutes. The slides were washed with PBS at 10 minutes, blocked with 2% goat serum and 1% BSA in PBS for 1 hour at RT, and permeabilized in 0.2% Triton-X100 in 2% goat serum and 1% BSA in PBS for 30 minutes. The slides were stained by incubation with Alexa568-coupled phalloidin diluted 1:40 in PBS for 1 hour, excess fluorochrome removed by 3 × 15 minutes rinse with 50 mL PBS, and counterstained with DAPI. The slides were mounted for microscopy examination using FluorSave reagent (Calbiochem, Millipore, Billerica, MA) as mounting medium.

Proliferating Cell Nuclear Antigen Stain

The mouse terminal ileum tissues were stained with rabbit anti–proliferating cell nuclear antigen (PCNA) antibody (Abcam) using a previously published method.[35] After staining for PCNA, the sections were stained with DAPI and imaged with Zeiss inverted microscope (Zeiss, Toronto, Canada). PCNA-positive cells were counted by 2 blinded reviewers in a minimum of 5 villi per animal.

In Vivo Permeability Assays

In vivo permeability was assessed with permeation of fluorescein isothiocyanate-dextran, fluorescent microspheres, and bacterial translocation studies. For dextran studies, after an overnight fast with free access to water, mice were gavaged with 0.6 μg/kg fluorescein isothiocyanate-dextran (FD-4, 4 kD; Sigma-Aldrich, St. Louis, MO). Blood samples were collected at 4 hours after cardiac puncture, serum was centrifuged at 1957*g* in 4°C for 20 minutes. Fluorescence emission of the supernatant was measured using 488 nm laser on the Typhoon Variable Mode Imager (GE Healthcare Life Sciences).

For microsphere studies, mice were gavaged with a mixture containing 10^7 Fluoresbrite Yellow Green Microspheres with diameter of 0.5, 1.0, 2.0, 3.0, and 6.0 μm in 200 μL solution as previously described after an overnight fast.[36] Blood samples were collected 4 hours after administration of the beads. Whole-blood mixture was then centrifuged at 1250*g* in preheparinized tubes for 10 minutes at RT, and the plasma portion of the samples were removed and centrifuged at 1250*g* for 5 minutes before the flow cytometry analysis. The remaining buffy coat and hematocrit of the samples were lysed with 5 mL lysing buffer (4.15 g NH_4Cl, 0.84 g $NaHCO_3$, 1 mL 0.5 mM EDTA at pH 8, and 500 mL

ddH_2O) at RT, mixed, and centrifuged at 1250*g* for 5 minutes at 4°C, the supernatant was discoarded and repeated × 2. The white blood cell pellet was resuspended in 400 μL of 0.03% PBS with fetal bovine albumin. The plasma and white blood cell pellet samples were analyzed with flow cytometry for determination of microsphere counts.

For bacterial translocation studies, mice were gavaged with 1×10^{10} colony forming units of green fluorescent protein–labeled *E. coli* suspended in 0.17 mL Luria broth. After 20 hours, spleen and liver samples were collected under sterile surgical conditions. The organs were suspended in preweighed tubes with Luria broth, homogenized with sterile RNase-free plastic pestles for 5 to 10 minutes. The homogenate was centrifuged, and the supernatant was plated onto 4 plates at varying dilutions for culture.

Confocal Laser Endomicroscopy and Confocal Microscopy

Confocal laser endomicroscopy of the mouse ileum and confocal microscopy of whole-mount mouse intestinal tissues for determination of epithelial gap density were performed using previously described methods.[37] Cell culture and human and mouse intestinal slides were imaged using a spinning disc confocal microscope (Quorum Technologies, Inc., Guelph, Canada) using previously described methods.[37]

Electron Microscopy

Control and nigericin-treated T84 cells were fixed with 2% (vol/vol) glutaraldehyde buffered with 0.1 M cacodylate–HCl at pH 7.4 overnight 4°C. After fixation, they were washed in cacodylate buffer and postfixed for 2 hours in 1% (wt/vol) osmium tetroxide and then rewashed in cacodylate buffer. After dehydration in a graded series of ethanol concentrations, specimens were placed in several washes of propylene oxide and subsequently embedded in Epoxy resin (EPON 12, Momentive Specialty Chemicals Inc., Columbus, OH). Ultrathin sections were contrasted with uranyl acetate and lead citrate and examined with a Hitachi 7650 transmission electron microscope (Hitachi High Technologies America, Dallas, TX) at an accelerating voltage of 60 kV. Fields of view were recorded and printed at final magnifications between 1000 and 4800, calibrated with the aid of carbon-grating replicas.

Statistical Analyses

Wilcoxon rank-sum test computed by GraphPad (La Jolla, CA) Prism 4 was used to compare the samples. Two-sided *P* values of <0.05 were considered to be significant. Bonferroni adjustments were made for multiple comparisons.

RESULTS

Caspase-1–mediated IEC Extrusion Results in Breaches in the Epithelial Monolayer

To investigate the morphology of caspase-1–induced IEC extrusion, we applied nigericin, a well-established Nlrp3-dependent

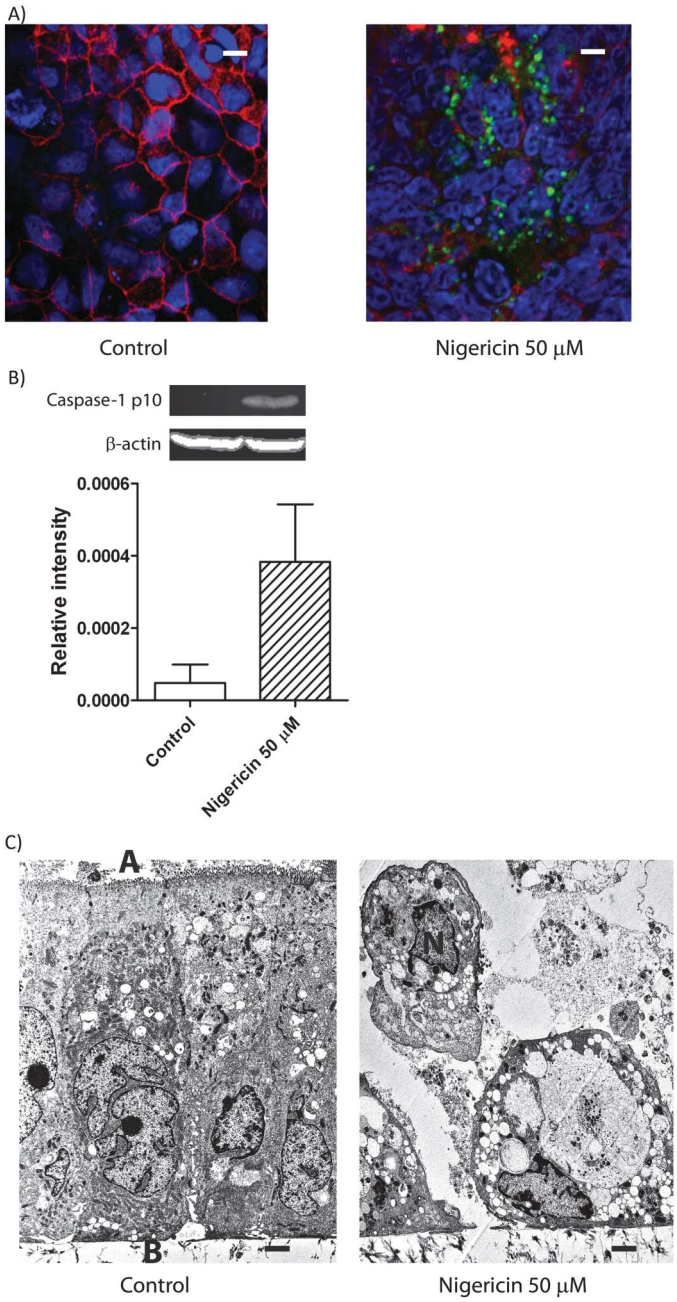

FIGURE 1. Caspase-1 activation of IECs induced cell extrusion in the polarized T84 monolayer. A, Representative FLICA-1 staining (green) of activated caspase-1 in nigericin-treated (50 μM) cultured T84 cells. Red, ZO-1 stain; blue, DAPI; green, FLICA-1 stain (scale bars, 50 μm). B, Increased active caspase-1 (p10) expression in nigericin-treated (50 μM) T84 cells. C, Transmission electron microscopy appearance of T84 cells treated with nigericin: chromatin condensation around the nuclear membrane, small and large clear vacuoles with dense bodies in the cytoplasm, and intact mitochondria with increase in the matrix density. A, apical surface; B, basal surface; N, nucleus (scale bars, 2 μm).

inflammasome activator,[38] to polarized T84 monolayers. Using FLICA-1 staining, we observed increased activated caspase-1 and cell extrusion in monolayers at 3 hours after treatment (Fig. 1A). Active caspase-1 expression in nigericin-treated T84 cells was confirmed by Western blot analysis (Fig. 1B). The morphological appearance of extruded cells from the monolayers by transmission electron microscopy revealed distinct chromatin condensation in the nuclei, intact mitochondria, and small or large clear vacuoles in the cytoplasm (Fig. 1C).

To determine whether this form of cell extrusion results in loss of barrier function,[4] we measured the transepithelial electrical resistance (TER). Following nigericin exposure, dose-dependent barrier dysfunction developed, which was abrogated by pretreatment with a selective, potent, and irreversible caspase-1 inhibitor Ac-YVAD-CMK[39] at 3 hours (Fig. 2A) and after overnight treatment (Fig. 2B). Given that the breach in the T84 monolayers appeared to be 1 to 2 μm in diameter on transmission electron microscopy images, we evaluated the epithelial integrity to microparticles (1-μm Fluoresbrite Yellow Green Microspheres) and microbes (*E. coli* TMW2.497) using the lowest dose of nigericin treatment. Movements of microspheres and *E. coli* from the upper chamber through the monolayer to the lower chamber of the Transwell were observed (Fig. 2C). Fluoresbrite microspheres and *E. coli* TMW2.497 were recovered in the media from basolateral well.

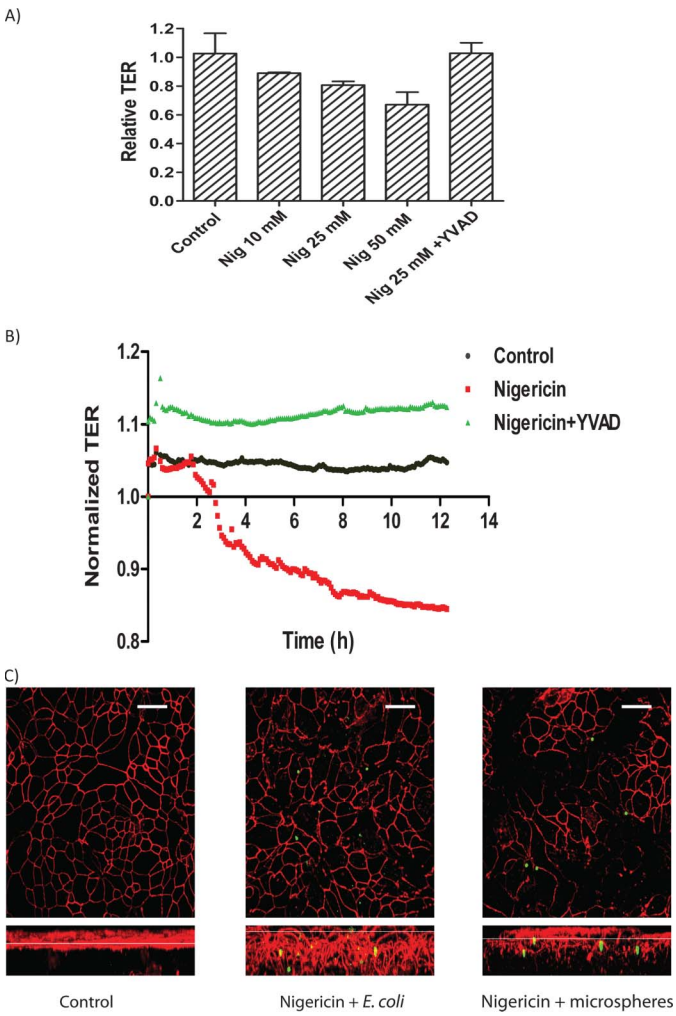

FIGURE 2. Altered permeability of the polarized monolayers after caspase-1 activation. A, Dose-dependent reduction in TER (±SD) of T84 monolayers treated with nigericin, reversed with Ac-YVAD-CMK (at nigericin 25 μM). B, Time-dependent reduction in TER as measured by ECIS of T84 monolayers treated with nigericin, reversed with Ac-YVAD-CMK (at nigericin 25 μM). C, Movements of Fluoresbrite Yellow Green microspheres and *Escherichia coli* TMW2.497 across the monolayer treated with nigericin 10 μM overnight. Red, ZO-1 stain; center image green,1-μm microspheres; right image green, *E. coli* TMW2.497 (scale bars, 50 μm). Data are representative of 3 independent experiments.

Modulation of Caspase-1 on Cell Extrusion and Epithelial Integrity In Vivo

To understand the effect of caspase-1–induced IEC extrusion on the permeability of the intestine in vivo, we first examined whether increased cell extrusion (as measured by increased density of epithelial gaps) observed in the IL-10 KO compared with 129/SvEv wild-type (WT) mice was due to increased caspase-1 activation.[32] Increased active caspase-1 expression in the small intestine of IL-10 KO mice was seen on Western blot analysis (Fig. 3A) and was confirmed with increased active IL-1β expression by enzyme-linked immunosorbent assay (Fig. 3B). To determine if reduced cellular proliferation in IL-10 KO contributed to the differences in epithelial gap densities observed, we stained the intestinal samples from 2 mouse strains with PCNA. IL-10 KO had a 38% reduction in cellular proliferation compared with WT mice (Fig. 3C, D).

The effect of increased IEC extrusion on intestinal permeability was investigated with permeation of macromolecules (dextran) and microparticles (Fluoresbrite Yellow Green Microspheres) into the blood and with translocation of microbes (*E. coli* TMW2.497) to liver and spleen in the IL-10 KO and WT mice. Increased IEC extrusion correlated with enhanced permeation of dextran (Fig. 4A) and 0.5-μm microspheres (Fig. 4B) into the blood, and translocation of *E. coli* (Fig. 4C) as determined by tissue cultures. Confocal microscopy of ileal tissues from mice gavaged with green fluorescent protein–labeled *E. coli* revealed the presence of bacteria near extrusion zones in the IL-10 KO intestine (Fig. 4D).

To evaluate the effect of caspase-1 inhibition on IEC extrusion over time in vivo, we treated the IL-10 KO mice with a selective caspase-1 inhibitor Ac-YVAD-CMK (10 mg/kg) over 4, 7, and 10 days (5 times the mean lifespan of rodent enterocytes[40]) through intraperitoneal injections. The control IL-10 KO group received 10 days of equal volume of 2% (vol/vol) dimethyl sulfoxide. Time-dependent reduction in IEC extrusion as measured by a decrease in epithelial gap density resulted (Fig. 5A) in the IL-10 KO mice treated with YVAD. The reduction in gap density was accompanied by normalization of permeation of oral gavaged 0.5-μm inert latex microspheres into blood at day 7 (Fig. 5B).

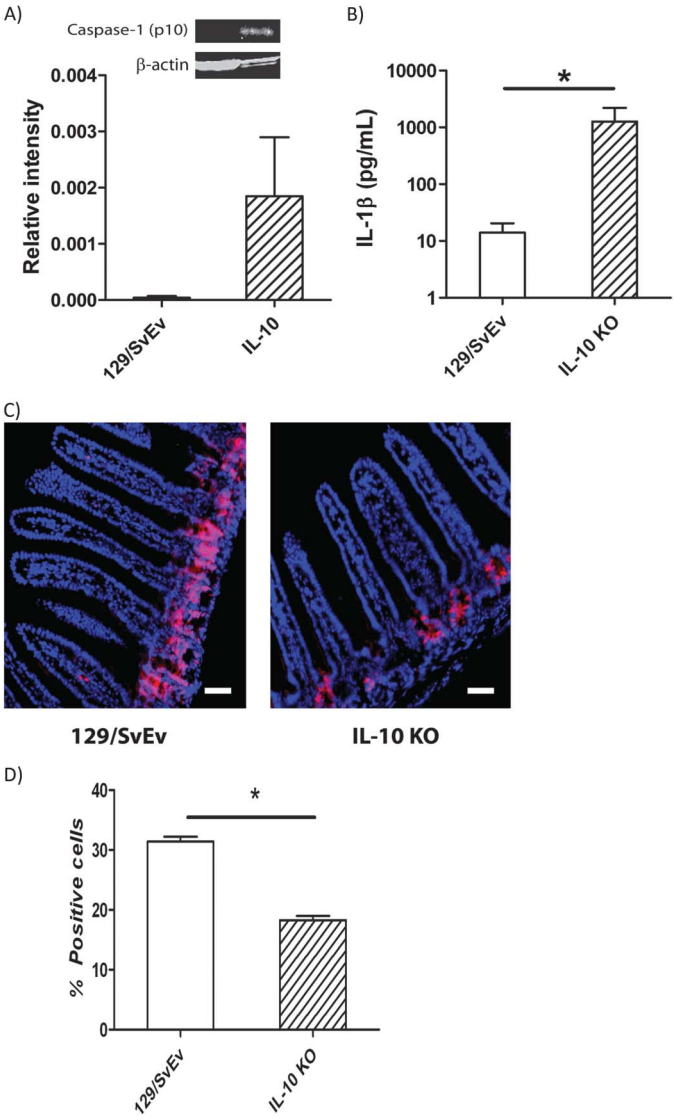

FIGURE 3. Increased caspase-1 activation in IL-10 KO compared with WT mice. A, Increased active caspase-1 (p10) expression in the IL-10 KO by Western blot analysis. B, Increased active IL-1β in intestinal tissue of the IL-10 KO (N = 5). C, representative images of PCNA-stained intestinal sections from WT and IL-10 KO mice (scale bars, 50 μm). D, Number of positive PCNA staining cells per crypt of rodent intestinal tissue. *$P < 0.05$.

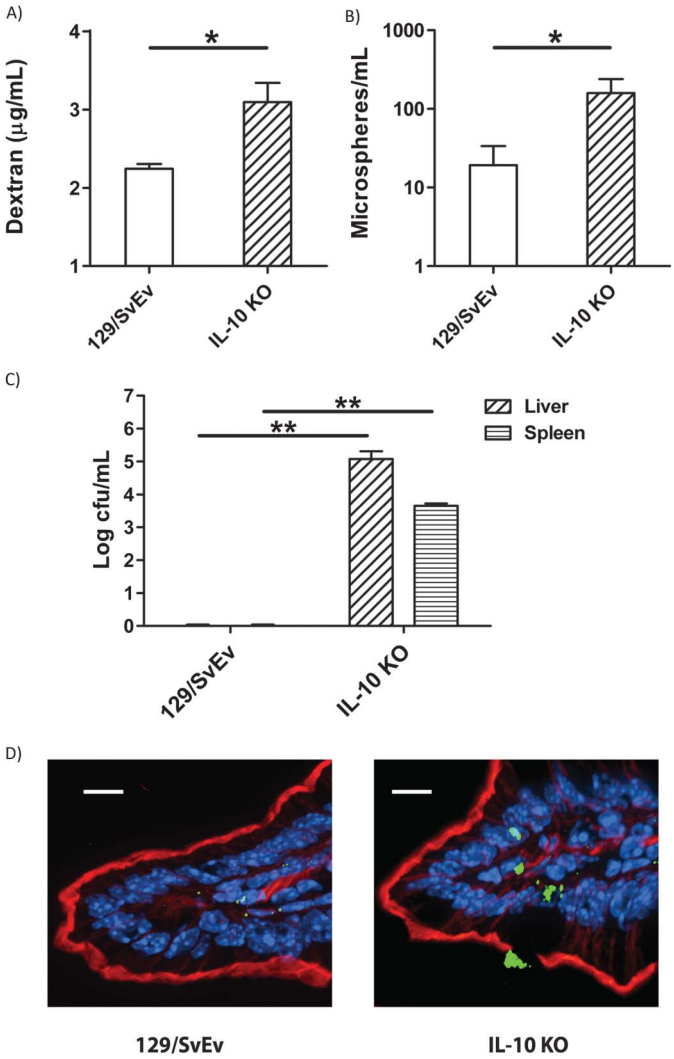

FIGURE 4. Increased permeability to luminal microparticles and microbes in the IL-10 KO mice. A, Permeation of orally administered fluorescein isothiocyanate-dextran into blood samples (N = 4). B, Presence of orally administered 0.5-μm Fluoresbrite Yellow Green microspheres in blood samples (N = 6). C, Translocation of *Escherichia coli* TMW2.497 to liver and spleen (N = 4). D, Representative images of *E. coli* TMW2.497 entering an extrusion zone in the mouse intestine. *$P < 0.05$; **$P < 0.01$. CFU, colony forming units.

The effect of caspase-1 activation on IEC extrusion and epithelial integrity was examined with the administration of *P. aeruginosa* type IV pili[41]—an ICE protease–activating factor inflammasome activator that could be given orally to induce caspase-1 activation. We chose *P. aeruginosa* type IV pili because nigericin could not be administered orally and was associated with significant systemic toxicity. In WT mice that were oral gavaged with type IV pili (0.33 mg/kg) for 1 day, we observed an increase in IEC extrusion as measured by higher epithelial gap density compared with control mice gavaged with equal volume of saline (Fig. 5C).

Nonapoptotic IEC Extrusion in the Human Intestine Is Mediated by Caspase-1 Activation

To explore whether caspase-1 activation of IECs represents a major mechanism of cell extrusion in humans, we collected mucosal biopsies and luminal aspirates from normal-appearing terminal ileum of patients with IBD and asymptomatic control patients. Mucosal biopsy samples were stained with FLICA-1 and FLICA-3&7 to identify IECs positive for activated caspase-1 (pyroptotic) or caspase-3&7 (apoptotic) stains (Fig. 6A). The ratio of positively stained caspase-1 to caspase-3&7 cells in control patients was 1.16:1; which was increased to 1.7:1 in patients with IBD (Fig. 6B). For the analysis of luminal aspirates, control

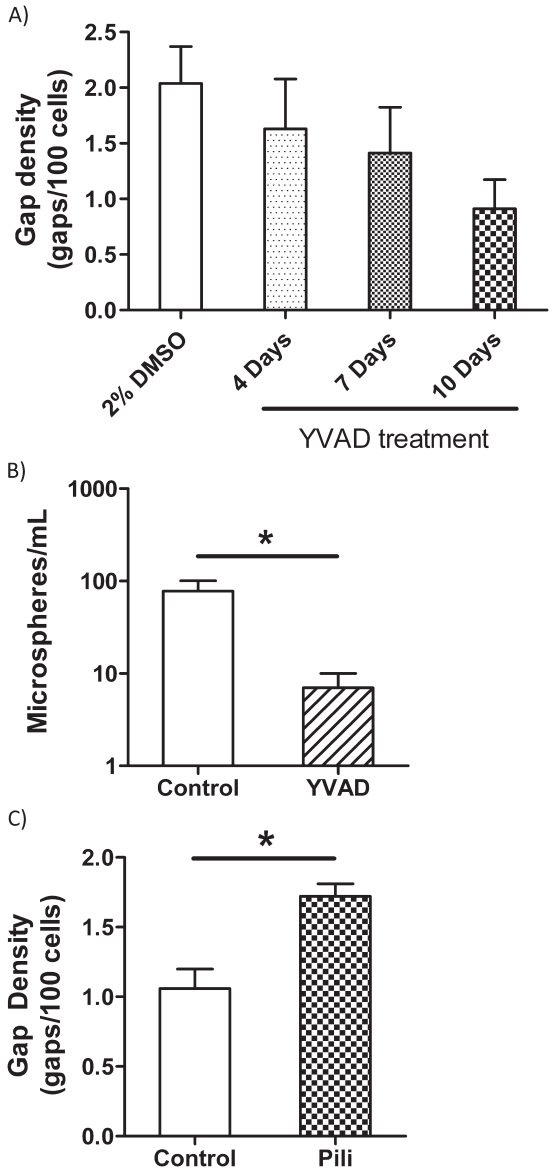

FIGURE 5. Modulation of caspase-1 on IEC extrusion and permeation of microspheres in vivo. A, Treatment with Ac-YVAD-CMK 10 mg/kg on IEC extrusion in IL-10 KO mice as measured by epithelial gap density using confocal endomicroscopy over time (N = 5). B, Presence of orally administered 0.5-μm Fluoresbrite Yellow Green microspheres in the blood samples of IL-10 KO mice (N = 6). C, Oral gavage of type IV pili of *Pseudomonas aeruginosa* 0.33 mg/kg for 1 day on IEC extrusion in WT mice (N = 3) as measured by gap density. *$P < 0.05$.

patients had insufficient material for cytology block preparation. In patients with IBD, the total number of nucleated cells seen on cytology blocks ranged from 12 to 155 cells, with IECs accounting from 41% to 100% of the cells (Fig. 6C). We quantitated the total number of extruded cells in the luminal aspirates collected on the filter: significantly higher cell counts were observed in luminal aspirates from patients with IBD compared with control patients (Fig. 6D). The extruded cells and cellular debris were stained with FLICA for activated caspase-1 and caspase-3&7. The images of FLICA-stained luminal aspirates were scored based on the intensity of the caspase staining of cells and cellular debris present on the 2 membranes, similar to a grading scale used for histologic samples. Each image was assigned a score of 0 to 4 depending on the intensity of stain and the number of stained cells or cellular debris. Using this scoring system, the ratio of positively stained caspase-1 to caspase-3&7 cells in control patients was approximately 1:1, which was increased to 2:1 in patients with IBD (Fig. 6E).

The expression of active IL-1β in mucosal biopsy samples was measured with enzyme-linked immunosorbent assay and was significantly higher in patients with IBD (Fig. 7A). Increased expression of active caspase-1 and IL-1β in mucosal biopsy samples were confirmed with Western blot analysis (Fig. 7B, C). Taken together, these results suggest that caspase-1 activation represents a significant mechanism of IEC extrusion in healthy human intestine and seems to be responsible for the majority of increase in cell extrusion observed in patients with IBD.

DISCUSSION

In this study, we described an inflammatory form of IEC extrusion mediated by caspase-1 activation that leads to breaches in the epithelium in vitro and in vivo. This form of IEC extrusion permitted the movement of microparticles and microbes across the polarized monolayers. IEC extrusion in the rodent intestine could be modulated by activation or inhibition of the caspase-1 enzyme. Increased IEC extrusion in the IL-10 KO mice was associated with increased permeation of macromolecules (dextran), microparticles, and translocation of commensal bacteria. Modulation of caspase-1 activity in vivo resulted in alterations in IEC extrusion with accompanying changes in epithelial integrity as measured by permeation of inert latex microspheres. Caspase-1–mediated IEC shedding could be observed in the small intestine of healthy individuals and patients with IBD, with pronounced increase in patients with IBD. Our experimental results provide fundamental new insights into the underlying mechanism of IEC extrusion previously reported to compromise epithelial integrity.[7]

Consistent with previous morphological analysis of duodenal aspirates showing extruded cells with features of pyroptosis and apoptosis,[7] our luminal aspirate studies revealed activation of both caspase-1 and caspase-3&7 in extruded cells. Our mucosal biopsy analysis findings are in agreement with a previous study where apoptosis was found in 44% of shedded IECs using activated caspase-3 staining of the human intestinal specimens.[6] In this study, we observed caspase-3&7 activation in 46% of IECs to be extruded.

The results of our analysis of extruded cells and biopsy samples from patient are complementary and consistent and are in agreement with previous studies of extruded IECs.[6] The luminal aspirates analysis may be limited by the fact that extruded IECs can break up into fragments after shedding; therefore, mucosal biopsy analysis results were essential to confirm the relative ratio of positively stained caspase-1 and caspase-3&7 cells. Because

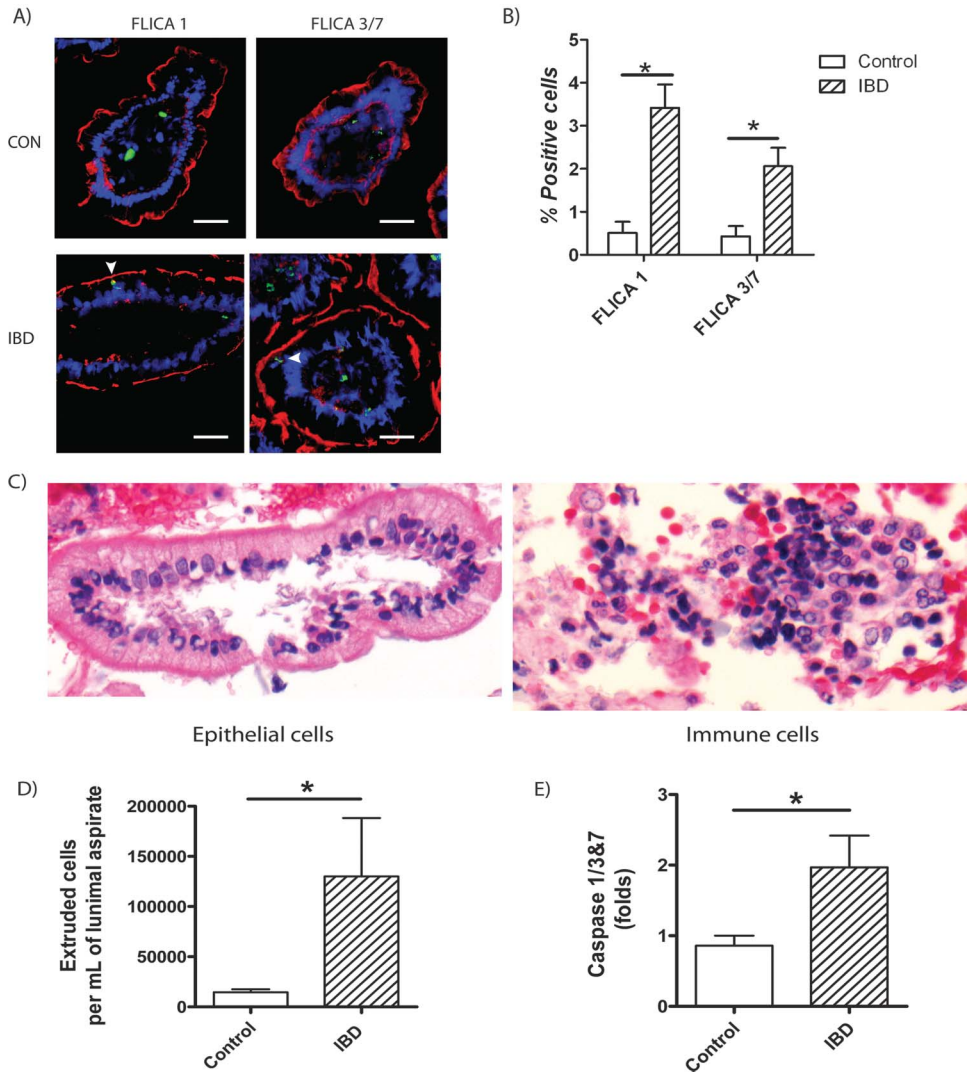

FIGURE 6. Caspase-1 and caspase-3&7 activation of IECs in patients. A, Representative activated caspase-1 and caspase-3&7 stains of mucosal biopsy samples, white arrowheads indicating positively stained IECs (scale bars, 50 μm). B, FLICA-1–stained or FLICA-3&7–stained cells normalized to the total number of epithelial cells (±SD) in mucosal biopsy samples in control patients (N = 3) and patients with IBD (N = 3). C, Representative epithelial and immune cells from cytology block prepared from luminal aspirates of patients with IBD (hematoxylin–eosin stain, magnification ×400). D, Number of extruded IECs (±SD) in luminal aspirates of control patients (N = 7) and patients with IBD (N = 11). E, The ratio of activated caspase-1–positive over caspase-3&7–positive extruded cells in the luminal aspirates. *$P < 0.05$.

caspase-1–mediated cell extrusion zones may be permeable to microbes, its dramatic rise in patients with IBD may contribute to the increased intramucosal and lymph node–associated bacterial burden observed in previous studies.[25–27] The barrier function in patients were not examined in the current study. Because the epithelial defects seem to permit the entry of microparticles and microbes, the appropriate test in patients to examine epithelial integrity will require rigorous validation studies. In addition, we have not investigated the closure or healing mechanism of the extrusion zone after caspase-1–mediated cell shedding, which is critical to define the loss of epithelial integrity observed. In apoptosis-induced cell extrusion, contraction of surrounding cells and reorganization of the tight junctions are required to prevent the loss of barrier function. Future studies to delineate the biochemical events of the cell shedding process in pyroptosis will facilitate our understandings of the role of tight-junction modifications, contractile proteins involved in extrusion, and the closure mechanism(s) in this form of cell extrusion. A basic understanding of the closure mechanism after caspse-1–mediated cell extrusion may be needed to facilitate the development of a proper test to assess the epithelial integrity in patients.

The morphological appearance of extruded cells by transmission electron microscopy is consistent with previous reports of pyroptotic cells (Fig. 1C)[8,16] and fits the description of the form of IEC extrusion associated with compromised epithelial integrity in humans.[7] The results of the TER study suggest that breaches in

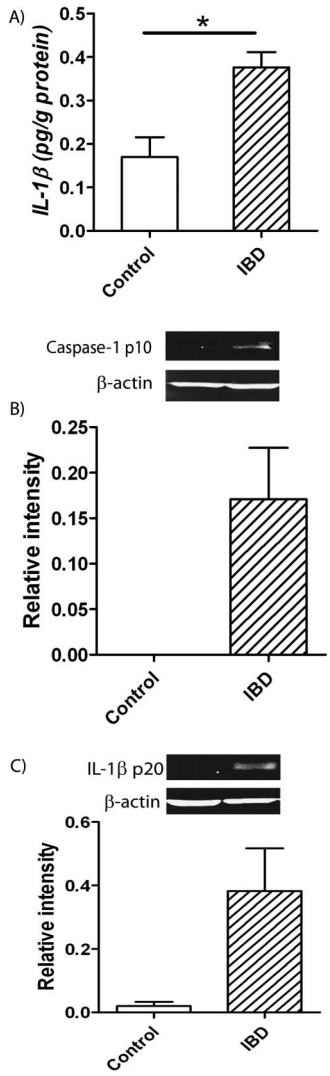

FIGURE 7. Activated caspase-1 and IL-1β expression in the mucosal tissue of asymptomatic control patients (N = 3) and patients with IBD (N = 3). A, Increased active IL-1β expression in patients with IBD compared with control patients as measured by enzyme-linked immunosorbent assay. B, Western blot analysis confirming increased expression of active IL-1β in terminal ileum of patients with IBD. C, Increased active caspase-1 (p10) expression in patients with IBD by Western blot analysis. *$P < 0.05$.

the epithelial lining induced by this form of cell extrusion is caspase-1 dependent. Our data further suggest that cell extrusion zones resulting from caspase-1 activation may provide entry sites for luminal microbes and antigens. Intracellular spaces as sites of microbial entry were observed in epithelia undergoing metabolic stress[42] and in a 3-dimensional coculture system of enterocytes, monocytes, and dendritic cells.[43] Here, we observed the development of similar barrier defects in the epithelium with inflammasome/caspase-1 activation in IECs alone.

In rodent models, modulation of caspase-1 activity altered IEC extrusion with associated changes in the integrity of the epithelial lining. Compared with apoptosis-mediated cell extrusion where barrier function of the epithelium is preserved,[2,44] we found that pyroptosis-mediated IEC extrusion introduced breaches in the epithelium that favored microbial and microparticle entry into the mucosa. Induction of pyroptosis with overnight treatment of type IV pili of *P. aeruginosa* resulted in higher IEC extrusion with accompanying increase in permeation of microspheres in the WT mice. Conversely, inhibition of caspase-1 activity in the IL-10 KO mice resulted in a time-dependent reduction in IEC extrusion as measured by epithelial gap density. Based on these observations, we estimated that time to achieve steady-state pharmacological activity (5 times the half-life) for colitis would be approximately 35 days for the IL-10 KO mice. Therefore, we chose to use permeation of oral gavaged latex microspheres—an assessment of epithelial integrity as a surrogate endpoint to study the physiological effect of reduced cell extrusion, rather than the usual clinical endpoint—improvement in colitis score. In our study, normalization of permeation of gavaged microspheres was achieved after 7 days of treatment.

Upstream to IL-1β, Nlrp3 is expressed in both immune and epithelial cells[45] and seems to play an important role in intestinal homeostasis.[21,46] Nlrp3$^{-/-}$ mice were more susceptible to experimental colitis induced by dextran sulfate sodium, 2,4,6-trinitrobenzene sulfonate (TNBS),[21,22]or *Citrobacter rodentium* infection.[47] Consistent with previous studies, our results indicate that caspase-1 activation induced IEC extrusion, mediated through either Nlrp3 or other pathways, maybe vital to intestinal homeostasis in health. IL-1β and IL-18 production resulting from caspase-1 activation has been shown to contribute to intestinal inflammation in some reports,[48,49] whereas other studies suggest that caspase-1 conferred protection against colitis and colitis-associated cancer.[21,22,35,50] The discrepancies in experimental results may due in part to the differences in genetic background, gender of the animals used, or variances in the microbial flora of the animal facilities.

In summary, the results of our study indicate that caspase-1 activation of IECs can induce cell extrusion that contributes to the development of barrier dysfunction in the intestinal epithelium, which may favor microbial entry into the mucosa. This form of cell extrusion seems to be the mechanism responsible for shedding events previously observed to introduce breaches in the epithelial lining.

ACKNOWLEDGMENTS

The authors are grateful to Ms. Theresa Kay, Ms. Stephanie Mah, and Mr. Harsh Thaker for their assistance with the experiments. The authors also thank Mr. Richard Vriend for his excellent preparation of the transmission electron microscopy images.

Author Contributions: J. J. Liu, E. M. Davis, D. Muruve, K. L. Madsen, R. T. Irvin: *conception and design of the study*. J. J. Liu, E. M. Davis, E. Wine, Y. Lou, J. K. Rudzinski, M. Alipour, P. Boulanger, A. L. Thiesen, C. Sergi, R. N. Fedorak, D. Muruve, K. L. Madsen, R. T. Irvin: generation, collection, assembly, analysis and/or interpretation of data. J. J. Liu, E. M. Davis, E. Wine, Y. Lou, J. K. Rudzinski, M. Alipour,

R. T. Irvin: drafting or revision of the manuscript. J. J. Liu, E. M. Davis, E. Wine, Y. Lou, J. K. Rudzinski, M. Alipour, P. Boulanger, A. L. Thiesen, C. Sergi, R. N. Fedorak, D. Muruve, K. L. Madsen, R. T. Irvin: approval of the final version of the manuscript.

REFERENCES

1. Mayhew TM, Myklebust R, Whybrow A, et al. Epithelial integrity, cell death and cell loss in mammalian small intestine. *Histol Histopathol.* 1999;14:257–267.
2. Rosenblatt J, Raff MC, Cramer LP. An epithelial cell destined for apoptosis signals its neighbors to extrude it by an actin- and myosin-dependent mechanism. *Curr Biol.* 2001;11:1847–1857.
3. Watson AJ, Chu S, Sieck L, et al. Epithelial barrier function in vivo is sustained despite gaps in epithelial layers. *Gastroenterology*. 2005;129:902–912.
4. Myklebust R, Mayhew TM. Further evidence of species variation in mechanisms of epithelial cell loss in mammalian small intestine: ultrastructural studies on the reindeer (Rangifer tarandus) and seal (Phoca groenlandica). *Cell Tissue Res.* 1998;291:513–523.
5. Sato T, Vries RG, Snippert HJ, et al. Single Lgr5 stem cells build crypt-villus structures in vitro without a mesenchymal niche. *Nature*. 2009;459:262–265.
6. Bullen TF, Forrest S, Campbell F, et al. Characterization of epithelial cell shedding from human small intestine. *Lab Invest.* 2006;86:1052–1063.
7. Shibahara T, Sato N, Waguri S, et al. The fate of effete epithelial cells at the villus tips of the human small intestine. *Arch Histol Cytol.* 1995;58:205–219.
8. Knodler LA, Vallance BA, Celli J, et al. Dissemination of invasive Salmonella via bacterial-induced extrusion of mucosal epithelia. *Proc Natl Acad Sci U S A.* 2010;107:17733–17738.
9. Thornberry NA, Bull HG, Calaycay JR, et al. A novel heterodimeric cysteine protease is required for interleukin-1 beta processing in monocytes. *Nature*. 1992;356:768–774.
10. Martinon F, Burns K, Tschopp J. The inflammasome: a molecular platform triggering activation of inflammatory caspases and processing of proIL-beta. *Mol Cell*. 2002;10:417–426.
11. Franchi L, Munoz-Planillo R, Nunez G. Sensing and reacting to microbes through the inflammasomes. *Nat Immunol.* 2012;13:325–332.
12. Kroemer G, Galluzzi L, Vandenabeele P, et al. Classification of cell death: recommendations of the Nomenclature Committee on Cell Death 2009. *Cell Death Differ.* 2009;16:3–11.
13. Fink SL, Bergsbaken T, Cookson BT. Anthrax lethal toxin and Salmonella elicit the common cell death pathway of caspase-1-dependent pyroptosis via distinct mechanisms. *Proc Natl Acad Sci U S A.* 2008;105:4312–4317.
14. Miao EA, Leaf IA, Treuting PM, et al. Caspase-1-induced pyroptosis is an innate immune effector mechanism against intracellular bacteria. *Nat Immunol.* 2010;11:1136–1142.
15. Labbe K, Saleh M. Cell death in the host response to infection. *Cell Death Differ.* 2008;15:1339–1349.
16. Bergsbaken T, Fink SL, Cookson BT. Pyroptosis: host cell death and inflammation. *Nat Rev Microbiol.* 2009;7:99–109.
17. Dinarello CA. Immunological and inflammatory functions of the interleukin-1 family. *Annu Rev Immunol.* 2009;27:519–550.
18. Mahida YR, Wu K, Jewell DP. Enhanced production of interleukin 1-beta by mononuclear cells isolated from mucosa with active ulcerative colitis of Crohn's disease. *Gut*. 1989;30:835–838.
19. Ligumsky M, Simon PL, Karmeli F, et al. Role of interleukin 1 in inflammatory bowel disease—enhanced production during active disease. *Gut*. 1990;31:686–689.
20. Brynskov J, Tvede N, Andersen CB, et al. Increased concentrations of interleukin 1 beta, interleukin-2, and soluble interleukin-2 receptors in endoscopical mucosal biopsy specimens with active inflammatory bowel disease. *Gut*. 1992;33:55–58.
21. Hirota SA, Ng J, Lueng A, et al. NLRP3 inflammasome plays a key role in the regulation of intestinal homeostasis. *Inflamm Bowel Dis.* 2010;17:1359–1372.
22. Zaki MH, Boyd KL, Vogel P, et al. The NLRP3 inflammasome protects against loss of epithelial integrity and mortality during experimental colitis. *Immunity*. 2010;32:379–391.
23. Villani AC, Lemire M, Fortin G, et al. Common variants in the NLRP3 region contribute to Crohn's disease susceptibility. *Nat Genet.* 2009;41:71–76.
24. Strober W, Fuss I, Mannon P. The fundamental basis of inflammatory bowel disease. *J Clin Invest.* 2007;117:514–521.
25. Swidsinski A, Ladhoff A, Pernthaler A, et al. Mucosal flora in inflammatory bowel disease. *Gastroenterology*. 2002;122:44–54.
26. Moussata D, Goetz M, Gloeckner A, et al. Confocal laser endomicroscopy is a new imaging modality for recognition of intramucosal bacteria in inflammatory bowel disease in vivo. *Gut*. 2011;60:26–33.
27. Keita AV, Salim SY, Jiang T, et al. Increased uptake of non-pathogenic E. coli via the follicle-associated epithelium in longstanding ileal Crohn's disease. *J Pathol.* 2008;215:135–144.
28. Duchmann R, Kaiser I, Hermann E, et al, Meyer zum Buschenfelde KH. Tolerance exists towards resident intestinal flora but is broken in active inflammatory bowel disease (IBD). *Clin Exp Immunol.* 1995;102:448–455.
29. Turner JR. Intestinal mucosal barrier function in health and disease. *Nat Rev Immunol.* 2009;9:799–809.
30. Guan Y, Watson AJ, Marchiando AM, et al. Redistribution of the tight junction protein ZO-1 during physiological shedding of mouse intestinal epithelial cells. *Am J Physiol Cell Physiol.* 2011;300:C1404–C1414.
31. Kiesslich R, Goetz M, Angus EM, et al. Identification of epithelial gaps in human small and large intestine by confocal endomicroscopy. *Gastroenterology*. 2007;133:1769–1778.
32. Liu JJ, Madsen KL, Boulanger P, et al. Mind the gaps: confocal endomicroscopy showed increased density of small bowel epithelial gaps in inflammatory bowel disease. *J Clin Gastroenterol.* 2011;45:240–245.
33. Giltner CL, van Schaik EJ, Audette GF, et al. The Pseudomonas aeruginosa type IV pilin receptor binding domain functions as an adhesin for both biotic and abiotic surfaces. *Mol Microbiol.* 2006;59:1083–1096.
34. Kilimann KV, Hartmann C, Vogel RF, et al. Differential inactivation of glucose- and glutamate dependent acid resistance of Escherichia coli TMW 2.497 by high-pressure treatments. *Syst Appl Microbiol.* 2005;28:663–671.
35. Dupaul-Chicoine J, Yeretssian G, Doiron K, et al. Control of intestinal homeostasis, colitis, and colitis-associated colorectal cancer by the inflammatory caspases. *Immunity*. 2010;32:367–378.
36. Limpanussorn J, Simon L, Dayan AD. Transepithelial transport of large particles in rat: a new model for the quantitative study of particle uptake. *J Pharm Pharmacol.* 1998;50:753–760.
37. Liu JJ, Rudzinski JK, Mah SJ, et al. Epithelial gaps in a rodent model of inflammatory bowel disease: a quantitative validation study. *Clin Transl Gastroenterol.* 2011;2:doi:10.1038/ctg.2011.2.
38. Mariathasan S, Weiss DS, Newton K, et al. Cryopyrin activates the inflammasome in response to toxins and ATP. *Nature*. 2006;440:228–232.
39. Garcia-Calvo M, Peterson EP, Leiting B, et al. Inhibition of human caspases by peptide-based and macromolecular inhibitors. *J Biol Chem.* 1998;273:32608–32613.
40. Weiser MM, Ryzowicz S, Soroka CJ, et al. Synthesis of intestinal basement membrane. *Immunol Invest.* 1989;18:417–430.
41. Arlehamn CS, Evans TJ. Pseudomonas aeruginosa pilin activates the inflammasome. *Cell Microbiol.* 2011;13:388–401.
42. Nazli A, Yang PC, Jury J, et al. Epithelia under metabolic stress perceive commensal bacteria as a threat. *Am J Pathol.* 2004;164:947–957.
43. Leonard F, Collnot EM, Lehr CM. A three-dimensional coculture of enterocytes, monocytes and dendritic cells to model inflamed intestinal mucosa in vitro. *Mol Pharm.* 2010;7:2103–2119.
44. Marchiando AM, Shen L, Graham WV, et al. The epithelial barrier is maintained by in vivo tight junction expansion during pathologic intestinal epithelial shedding. *Gastroenterology*. 2011;140:1208–1218 e1–2.
45. Kummer JA, Broekhuizen R, Everett H, et al. Inflammasome components NALP 1 and 3 show distinct but separate expression profiles in human tissues suggesting a site-specific role in the inflammatory response. *J Histochem Cytochem.* 2007;55:443–452.
46. Zaki MH, Lamkanfi M, Kanneganti TD. The Nlrp3 inflammasome: contributions to intestinal homeostasis. *Trends Immunol.* 2011;32:171–179.
47. Liu Z, Zaki MH, Vogel P, et al. Role of inflammasomes in host defense against Citrobacter rodentium infection. *J Biol Chem.* 2012;287:16955–16964.
48. Siegmund B, Lehr HA, Fantuzzi G, et al. IL-1 beta -converting enzyme (caspase-1) in intestinal inflammation. *Proc Natl Acad Sci U S A.* 2001;98:13249–13254.
49. Bauer C, Loher F, Dauer M, et al. The ICE inhibitor pralnacasan prevents DSS-induced colitis in C57BL/6 mice and suppresses IP-10 mRNA but not TNF-alpha mRNA expression. *Dig Dis Sci.* 2007;52:1642–1652.
50. Allen IC, TeKippe EM, Woodford RM, et al. The NLRP3 inflammasome functions as a negative regulator of tumorigenesis during colitis-associated cancer. *J Exp Med.* 2010;207:1045–1056.